ANL/ET/CP-97126

HIGH–TEMPERATURE COMPRESSIVE DEFORMATION OF Si_3N_4/BN FIBROUS MONOLITHS*

J. L. Routbort, K. C. Goretta, E. T. Park, and D. Singh
Energy Technology Division
Argonne National Laboratory, Argonne, IL 60439

J. Finch,+ J. Staehler,++ and L. Zawada
Materials and Manufacturing Directorate
AFRL/MLLN, Wright–Patterson Air Force Base, OH 45433
+Also with University of Dayton Research Institute
++Also with Systran

G. E. Hilmas
Advanced Ceramics Research
Tucson, AZ 85706
(Now with the University of Missouri at Rolla)

January 1999

Submitted to Proceedings of 23rd Cocoa Beach Meeting, Cocoa Beach, FL, January 25-28, 1999.

*Work supported by the Defense Advanced Research Projects Agency through a Department of Energy Interagency Agreement under Contract W-31-109-Eng-38 at Argonne National laboratory, and Agreement No. DE-A102-96CH10871 at Wright– Patterson Air Force Base.

HIGH–TEMPERATURE COMPRESSIVE DEFORMATION OF Si_3N_4/BN FIBROUS MONOLITHS

J. L. Routbort, K. C. Goretta, E. T. Park, and D. Singh
Energy Technology Division
Argonne National Laboratory, Argonne, IL 60439

J. Finch,+ J. Staehler,++ and L. Zawada
Materials and Manufacturing Directorate
AFRL/MLLN, Wright–Patterson Air Force Base, OH 45433
+Also with University of Dayton Research Institute
++Also with Systran

G. E. Hilmas
Advanced Ceramics Research
Tucson, AZ 85706

ABSTRACT

Fibrous monolithic Si_3N_4/BN (≈85 vol.% Si_3N_4/15 vol.% BN) and monolithic Si_3N_4 ceramics were compressed at a nearly constant strain rate ($\dot{\varepsilon}$) at 1200–1400°C in N_2. The $\dot{\varepsilon}$ range was ≈1×10^{-6} to 5×10^{-6} s^{-1}; the stress (σ) range was 37–202 MPa. The Si_3N_4 and the unidirectional fibrous monoliths that were oriented with the long axis of the Si_3N_4 cells parallel to the compression direction exhibited plasticity at 1300 and 1400°C, with $\dot{\varepsilon} \propto \sigma$. A 0/90° cross-ply Si_3N_4/BN laminate also exhibited significant plasticity, but it was weaker than the above-mentioned ceramics. The unidirectional fibrous monoliths that were compressed perpendicular to the cell direction fractured at ≈50 MPa in all tests. A ±45° laminate tested at 1300°C fractured at a stress of ≈40 MPa. Low fracture stress correlated with shear through BN layers.

INTRODUCTION

Fibrous monolithic ceramics, which generally consist of a strong ceramic cell surrounded by a weaker cell boundary, exhibit graceful failure [1-5]; in flexure, they splinter. Fibrous monoliths are produced from powders by conventional ceramic fabrication techniques, such as extrusion [1,2].

Several compositions of ceramics and cermets have been processed successfully in fibrous monolithic form [4]. The most thoroughly investigated fibrous monolith consists of Si_3N_4 cells and a continuous BN cell boundary [3-5]. Through appropriate selection of initial powders and extrusion and hot-pressing parameters, very tough final products are produced. The high toughness is due primarily to the presence of textured platelike BN grains.

The mechanical properties of Si_3N_4/BN fibrous monoliths have been studied extensively at both room and high temperatures [3-9]. Although elevated-temperature creep failures of ceramic composites often occur by shear [10], Si_3N_4/BN fibrous monoliths have not been tested in compressive or shear loading. We report here on initial tests of Si_3N_4/BN fibrous monolithic specimens that were compressed at 1200–1400°C in N_2. For comparison, Si_3N_4 specimens with a composition similar to that of the cell phase were also compressed.

EXPERIMENTAL DETAILS

Fabrication Procedures

The fibrous monoliths were fabricated from Si_3N_4/BN coextruded green filaments [2] that were 320–330 μm in diameter, flexible, and produced by melt coextrusion of a blend of ≈52 vol.% ceramic powder mixture in an ethylene-based copolymer binder [11]. The coextruded filaments contained nominally 85 vol.% core Si_3N_4 material (E-10, Ube Industries, Tokyo) and 15 vol.% BN cladding (HCP Grade, Advanced Ceramics Corporation, Cleveland). The Si_3N_4 was a sinterable composition, 92 wt.% commercial Si_3N_4 powder, 6 wt.% Y_2O_3, and 2 wt.% Al_2O_3.

Sheets of uniaxially aligned green filaments were produced by a winding operation that placed the coextruded filaments side-by-side on a cylindrical mandrel. The filaments were held in place with a spray adhesive that, upon drying, allowed the unidirectional sheets of green fibrous monolith to be removed from the mandrel. The sheets were stacked to fabricate the specimens [5]. Three laminated architectures were fabricated: 0°, 0/90°, and ±45°. The laminates were cut into the desired preform and warm pressed at 160°C to produce a solid green panel.

In this study, simple rectangular flat panels were fabricated for the property evaluations. The panels underwent a binder pyrolysis step that consisted of slow heating in flowing N_2 to 600°C over a period of 42 h. The Si_3N_4/BN panels were then hot pressed at 1740°C for 1 h under ≈28 MPa pressure. This procedure yielded fibrous-monolith billets that were >98% of their theoretical density. Pure Si_3N_4 billets were also hot pressed.

Creep Tests and Microstructural Analysis

Right parallelepiped specimens ≈3 x 3 x 5 mm were cut from the fibrous-monolith and Si_3N_4 billets with a slow-speed diamond-blade saw. The compression surfaces were polished to be flat and parallel. Five types of specimens were prepared (Fig. 1).

Each specimen was compressed at constant velocity between Si_3N_4 platens in an Instron Model 1125 universal tester [12]. The atmosphere was stagnant N_2, the temperature was 1200–1400°C, and the engineering strain rates ($\dot{\varepsilon}$) were $\approx 1 \times 10^{-6}$ to 5×10^{-6} s^{-1}. All compressive tests were completed within 10 h. For most tests, the specimen were unloaded and reloaded and at least two data points were taken.

The maximum strain (ε) was <0.04, but some specimens fractured during testing. Fracture surfaces and polished sections were examined by scanning electron microscopy (SEM). One as-received specimen was thermally etched to reveal the Si_3N_4 grain size.

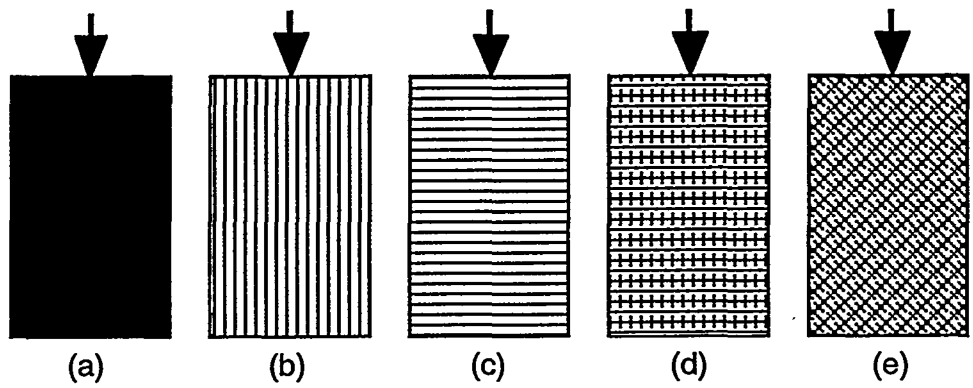

Fig. 1. Schematic diagram of specimens that were compressed: (a) Si_3N_4, (b) 0° laminate, (c) 0° laminate compressed at 90°, (d) laminate of alternating 0 and 90° layers, and (e) laminate of alternating + and –45° layers; arrows indicate compression direction.

RESULTS AND DISCUSSION

Key microstructural features of the monolithic Si_3N_4 and fibrous-monolithic Si_3N_4/BN are shown in Fig. 2. The Si_3N_4 grains in both types of specimens were generally elongated, with a maximum length of ≈5 μm. The cells of the fibrous monoliths were slightly distorted by hot pressing. Most cells were approximately hexagonal; the maximum cross-sectional dimension was ≈100–200 μm. The BN boundary layer was thin and nearly continuous.

A summary of the test data is shown in Table I. The selected range of $\dot{\varepsilon}$ proved to be too fast to allow appreciable plastic deformation at 1200°C. The Si_3N_4/BN specimens that were compressed perpendicular to the long cell direction were rather weak.

At 1300°C, the Si_3N_4 specimen appeared to achieve steady-state stresses; i.e., the stress saturated. The Si_3N_4/BN that was tested parallel to the long cell direction appeared to also achieve steady state, but at a stress (σ) that was ~20%

lower than that for the Si_3N_4. As was the case at 1200°C, the 90° specimen fractured at a $\sigma \approx 50$ MPa. The cross-ply laminates exhibited vastly different responses, with the ±45° laminate fracturing at low stress. The 0/90° laminate

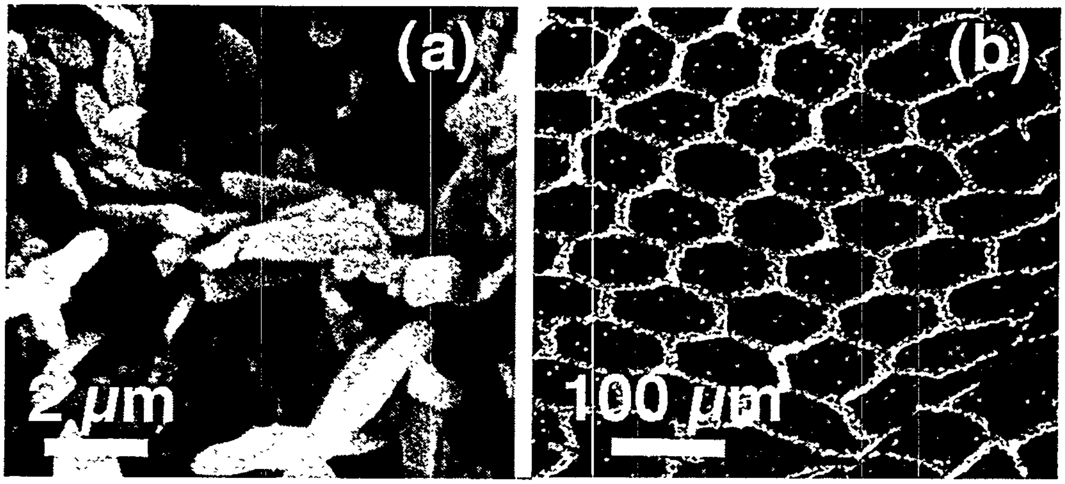

Fig. 2. SEM photomicrographs of (a) thermally etched Si_3N_4 cells in which grains are exposed and (b) Si_3N_4/BN fibrous monolith in which cell structure is evident: dark Si_3N_4 cells surrounded by lighter BN phase.

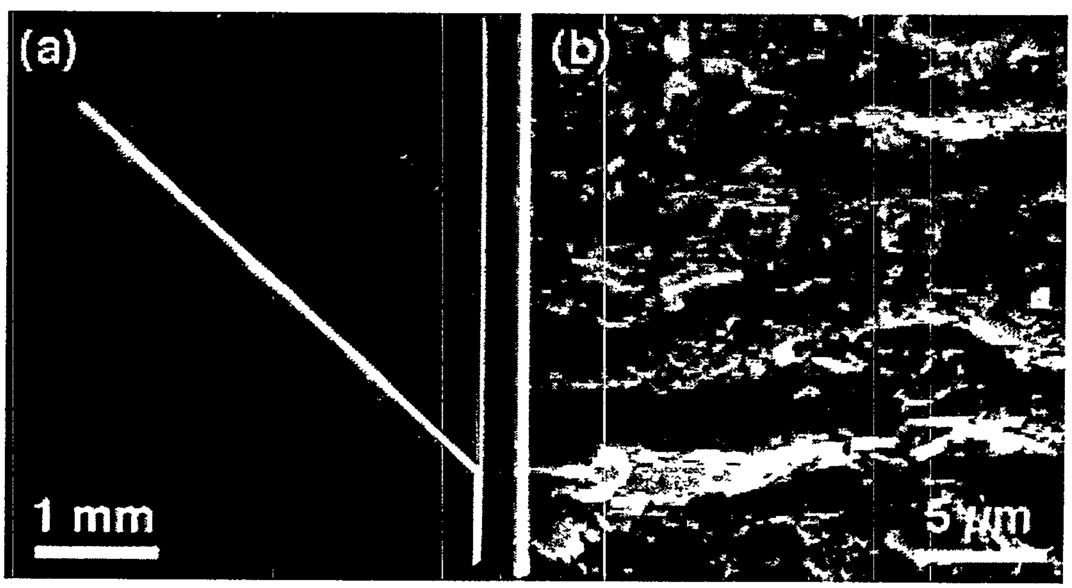

Fig. 3. SEM photomicrographs of fracture surface of ±45° Si_3N_4/BN laminate compressed at 1300°C: (a) low-magnification view and (b) higher-magnification view that shows platelike BN grains.

appeared to achieve steady-state creep at $\dot{\varepsilon} \approx 2 \times 10^{-6}$ s^{-1}, but upon retesting, fracturing became evident. Its maximum strength was approximately half that of the Si_3N_4 or the unidirectional fibrous monolith that was compressed parallel to the long cell direction. The ±45° laminates were very weak. Examination by SEM indicated that fracturing occurred between layers, through the BN boundary phase (Fig. 3).

At 1400°C, the Si_3N_4 and the 0° Si_3N_4/BN fibrous monolith exhibited very similar responses. The BN volume fraction was only ≈15% in the Si_3N_4/BN, and, because of the structure of the BN boundary phase, it probably offered some resistance to creep. Furthermore, the orientation of the BN boundary phase should have minimized a propensity to fracture. Nearly equal creep resistance was thus to be expected for these two ceramics; for both, $\dot{\varepsilon} \propto \sigma$, as would be expected for creep by diffusional flow [13,14]. The relatively low

Table I. Summary of compressive-test data for Si_3N_4 and Si_3N_4/BN specimens.

Specimen	T (°C)	$\dot{\varepsilon}$ (s-1)	σ (MPa)	Comments
Si_3N_4	1400	2×10^{-6}	46.3, 56.4	≈steady state
		4×10^{-6}	97.4	≈ steady state
Si_3N_4/BN (0°)	1400	1×10^{-6}	29.1	≈steady state
		2×10^{-6}	53.8	≈steady state
Si_3N_4/BN (90°)	1400	2×10^{-6}	52.0	≈steady state
		5×10^{-6}	52.8	fractured
Si_3N_4	1300	1×10^{-6}	87.4	≈steady state
		2×10^{-6}	202	≈ steady state
Si_3N_4/BN (0°)	1300	1×10^{-6}	57.5	steady state*
		2×10^{-6}	156.5	test suspended
Si_3N_4/BN (90°)	1300	1×10^{-6}	52.0	steady state**
		5×10^{-6}	52.8	fractured
Si_3N_4/BN (0/90°)	1300	2×10^{-6}	102	steady state**
		2×10^{-6}	92.2	fractured
Si_3N_4/BN (±45°)	1300	2×10^{-6}	41.7	fractured
(second sample)		2×10^{-6}	36.9	fractured
Si_3N_4	1200	1×10^{-6}	—	elastic
Si_3N_4/BN (0°)	1200	1×10^{-6}	209	fractured
Si_3N_4/BN (90°)	1200	2×10^{-6}	48.7	fractured

*Apparent steady state, but actual steady-state stress was probably higher.
**Apparent steady state, but slow fracture was likely [13].

steady-state stresses at 1300 and 1400°C, which imply fast creep rates, are probably due to a glass phase at the grain boundaries that was created by the oxide sintering aids [15,16].

The 90° Si_3N_4/BN specimen fractured, as at the lower test temperatures, at a stress of ≈50 MPa. Examinations by SEM indicated that the fracture propagated between the highly aligned platelike BN grains.

The tests were conducted over relatively short periods, with only one replicate specimen being tested; thus, the ascribed steady-state stresses must be considered as approximate only. Furthermore, the stress/strain curves for the fibrous monoliths (Fig. 4) exhibited significant serrations, probably from minor cracking of weakest sections, which further complicated identification of the steady-state stresses. Nevertheless, the following conclusions can be drawn from these tests:

Monolithic Si_3N_4 and fibrous monolithic Si_3N_4/BN that were compressed parallel to the long axis of the Si_3N_4 cells exhibited similar creep responses.

Fibrous monolithic Si_3N_4/BN compressed perpendicular to the long axis of the Si_3N_4 cells fractured at a stress of ≈50 MPa, independent of temperature and $\dot{\varepsilon}$ over the ranges examined. Fractures propagated through the weaker BN phase.

Cross-ply Si_3N_4/BN laminates were weakest in shear, with fractures propagating through the BN phase.

Boundaries between laminates, which consisted of essentially doubly thick layers of BN, proved to be the weakest regions in the Si_3N_4/BN fibrous monoliths.

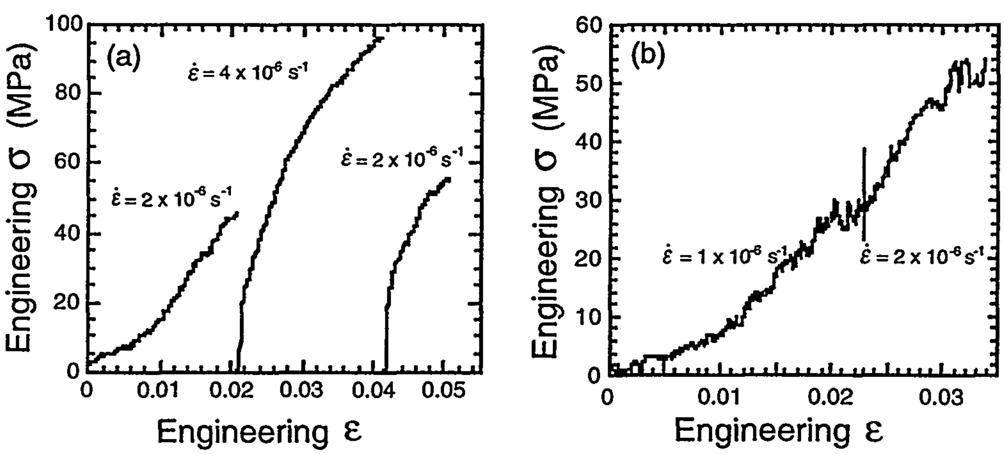

Fig. 4. Stress-vs.-strain curves at 1400°C for (a) Si_3N_4 and (b) unidirectional Si_3N_4/BN compressed parallel to the fibroid direction; the specimen was unloaded and reloaded twice in (a); in (b), the strain rate was changed during the test..

Our preliminary data and observations strongly suggest that laminate architecture should be tailored to match service stress states. The stresses imposed by our tests to date were relatively large. Lower-stress creep tests, conducted at constant σ rather than constant $\dot{\varepsilon}$, are in progress. The new tests should more accurately probe the performance of Si_3N_4/BN fibrous monoliths in applications.

SUMMARY

Fibrous monolithic Si_3N_4/BN and Si_3N_4 ceramics were compressed at 1200–1400°C in N_2. The unidirectional fibrous monoliths that were oriented with the long axis of the Si_3N_4 parallel to the compression direction exhibited a creep response similar to that of the Si_3N_4. Both ceramics exhibited steady-state creep at 1300 and 1400°C. A 0/90° cross-ply Si_3N_4/BN laminate also exhibited significant plasticity at 1300°C, but was weaker than these ceramics. The unidirectional fibrous monoliths that were compressed perpendicular to the long axis of the Si_3N_4 cells fractured at ≈50 MPa in all tests. The ±45° laminate tested at 1300°C fractured at a stress of ≈40 MPa. Low fracture stress correlated with shear through BN layers.

ACKNOWLEDGMENTS

This work was supported by the Defense Advanced Research Projects Agency through a Department of Energy Interagency Agreement under Contract W-31-109-Eng-38 at Argonne National laboratory, and Agreement No. DE-A102-96CH10871 at Wright–Patterson Air Force Base. G. E. Hilmas is now with the University of Missouri at Rolla.

REFERENCES

1. W. S. Coblenz, "Fibrous Monolithic Ceramic and Method for Production," U.S. Patent 4,772,524, Sept. 20, 1988.
2. D. Popovic, J. W. Halloran, G. E. Hilmas, G. A. Brady, S. Somas, A. Bard, and G. Zywicki, "Process for Preparing Textured Ceramic Composites," U.S. Patent 5,645,781, July 8, 1997.
3. G. Hilmas, G. A. Brady, U. Abdali, G. Zywicki, and J. Halloran, "Fibrous Monoliths: Non-brittle Fracture from Powder-processed Ceramics," Mater. Sci. Eng. **A195**, 263-68 (1995).
4. D. Kovar, B. H. King, R. W. Trice, and J. W. Halloran, "Fibrous Monolithic Ceramics," J. Am. Ceram. Soc. **80**, 2471-87 (1997).
5. G. A. Danko, G. E. Hilmas, J. W. Halloran, and B. King, "Fabrication and Properties of Quasi-isotropic Silicon Nitride–Boron Nitride Fibrous Monoliths," Ceram. Eng. Sci. Proc. **18** [3], 607-13 (1997).
6. D. Popovich, G. A. Danko, G. E. Hilmas, K. Stuffle, B. H. King, G. A. Brady, R. W. Trice, and J. W. Halloran, "Fibrous Monoliths: Room- and High-temperature Non-brittle Fracture from Powder Processed Ceramics," Ceram. Eng. Sci. Proc. **17** [3], 278-286 (1996).

7. D. Kovar, M. D. Thouless, and J. W. Halloran, "Crack Deflection and Propagation in Layered Silicon Nitride/Boron Nitride Ceramics," J. Am. Ceram. Soc. **81**, 1004-12 (1998).
8. S. W. Lee and D. K. Kim, "High Temperature Characteristics of Si_3N_4/BN Fibrous Monolithic Ceramics," Ceram. Eng. Sci. Proc. **18** [4], 481-86 (1997).
9. L. Zawada, AFRL/MLLN, Wright–Patterson Air Force Base, unpublished information (1998).
10. B. G. Nair, "High-temperature Rheology of a Continuous-fiber-reinforced Glass-ceramic Composite (Silicon Carbide/Anorthite)," Ph.D. Thesis, University of Wisconsin–Madison (1998).
11. G. A. Brady, G. E. Hilmas, and J. W. Halloran, "Forming Textured Ceramics by Multiple Coextrusion," pp. 609-14 in *Ceramic Transactions, Vol. 51, Ceramic Processing Science and Technology*. Edited by H. Hausner and G. Messing. American Ceramic Society, Westerville, OH, 1995.
12. J. L. Routbort, "Work Hardening and Creep of MgO," Acta Metall. **27**, 649-661 (1979).
13. A. G. Evans and T. G. Langdon, "Structural Ceramics," Prog. Mater. Sci. **21**, 171-441 (1976).
14. W. R. Cannon and T. G. Langdon, "Review: Creep of Ceramics, Part 1 Mechanical Characteristics," J. Mater. Res. **18**, 1-50 (1983).
15. G. Ziegler, J. Heinrich, and G. Wötting, "Review: Relationships between Processing, Microstructure and Properties of Dense and Reaction-bonded Silicon Nitride," J. Mater. Sci. **22**, 3041-86 (1987).
16. A. R. de Arellano-López, B. I. Smirnov, K. C. Goretta, and J. L. Routbort, "Creep of an Al_2O_3-SiC(Whisker)-TiC(Particle) Composite," Mater. Sci. Eng. **A252**, 93-97 (1998).